

Structure of Pb²⁺/deprotonated dGMP complexes in the gas phase: a combined MS-MS/IRMPD spectroscopy/Ion Mobility study.

*Jean-Yves Salpin^{*1,2}, Luke MacAleese^{*3,4}, Fabien Chiro^{5,6}, Philippe Dugourd^{3,4},*

1) Université d'Evry Val d'Essonne – Laboratoire Analyse et Modélisation pour la Biologie et l'Environnement – Boulevard François Mitterrand – 91025 Evry – France
2) CNRS- UMR 8587.

3) Université Lyon 1– Institut Lumière Matière, 5 rue de la Doua, 69622 Villeurbanne cedex – France

4) CNRS- UMR 5306.

5) Université Lyon 1 – Institut des Sciences Analytiques, 5 rue de la Doua, 69100 Villeurbanne – France

6) CNRS- UMR 5280

Supporting information

1S. Low energy CID spectrum of the [Pb(GMP)-H]⁺ complex recorded at 30 eV (laboratory frame).

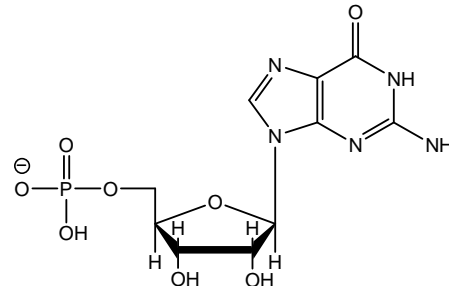
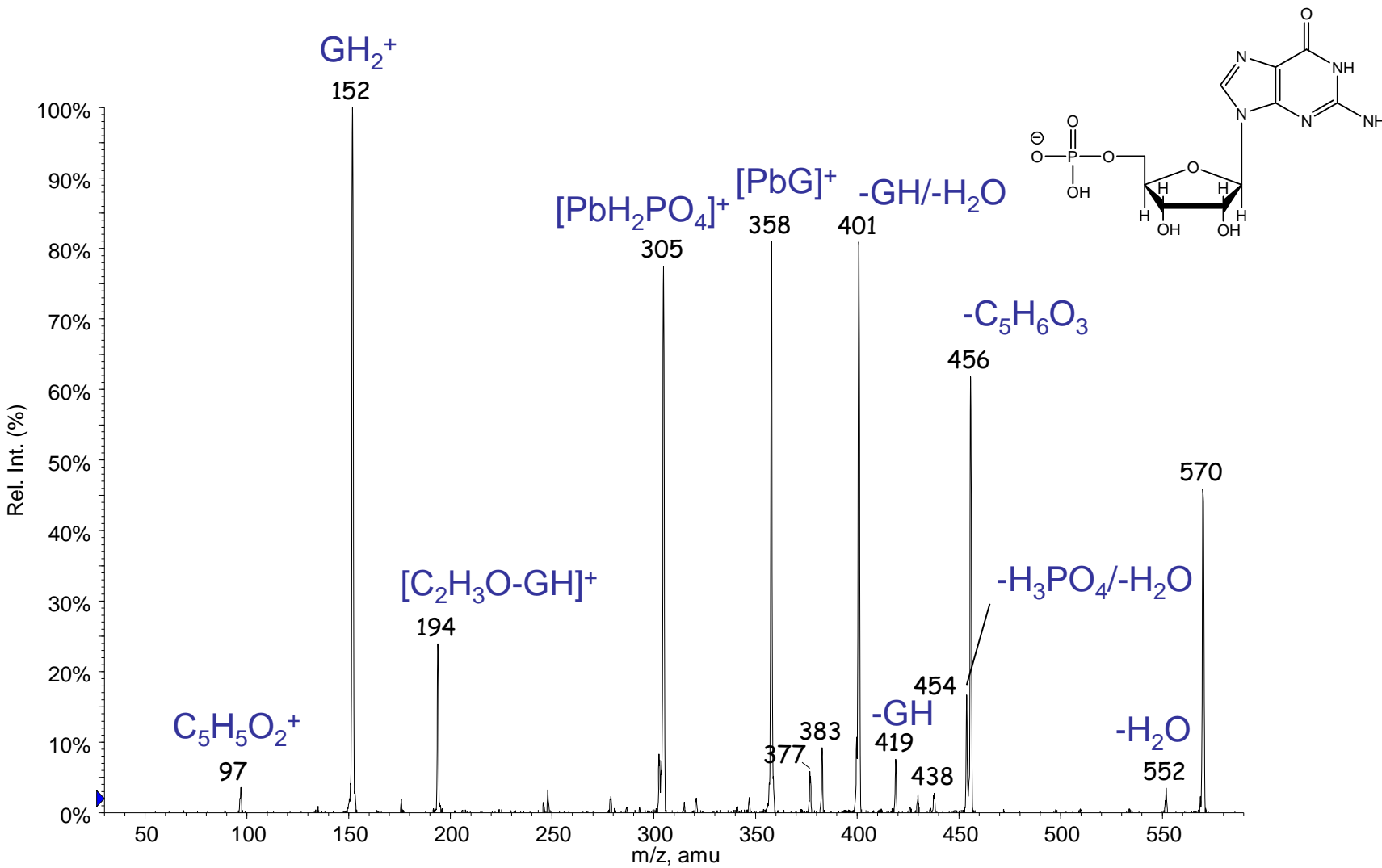
2S. Structure and geometrical details of the various structures optimized for the [Pb(dGMP)-H]⁺ complex

3S. Total energy and ZPE (Hartree) of the various structures considered

4S. DFT-computed IR absorption spectra for the [Pb(dGMP)-H]⁺ structures. The experimental IRMPD spectrum is overlayed in grey.

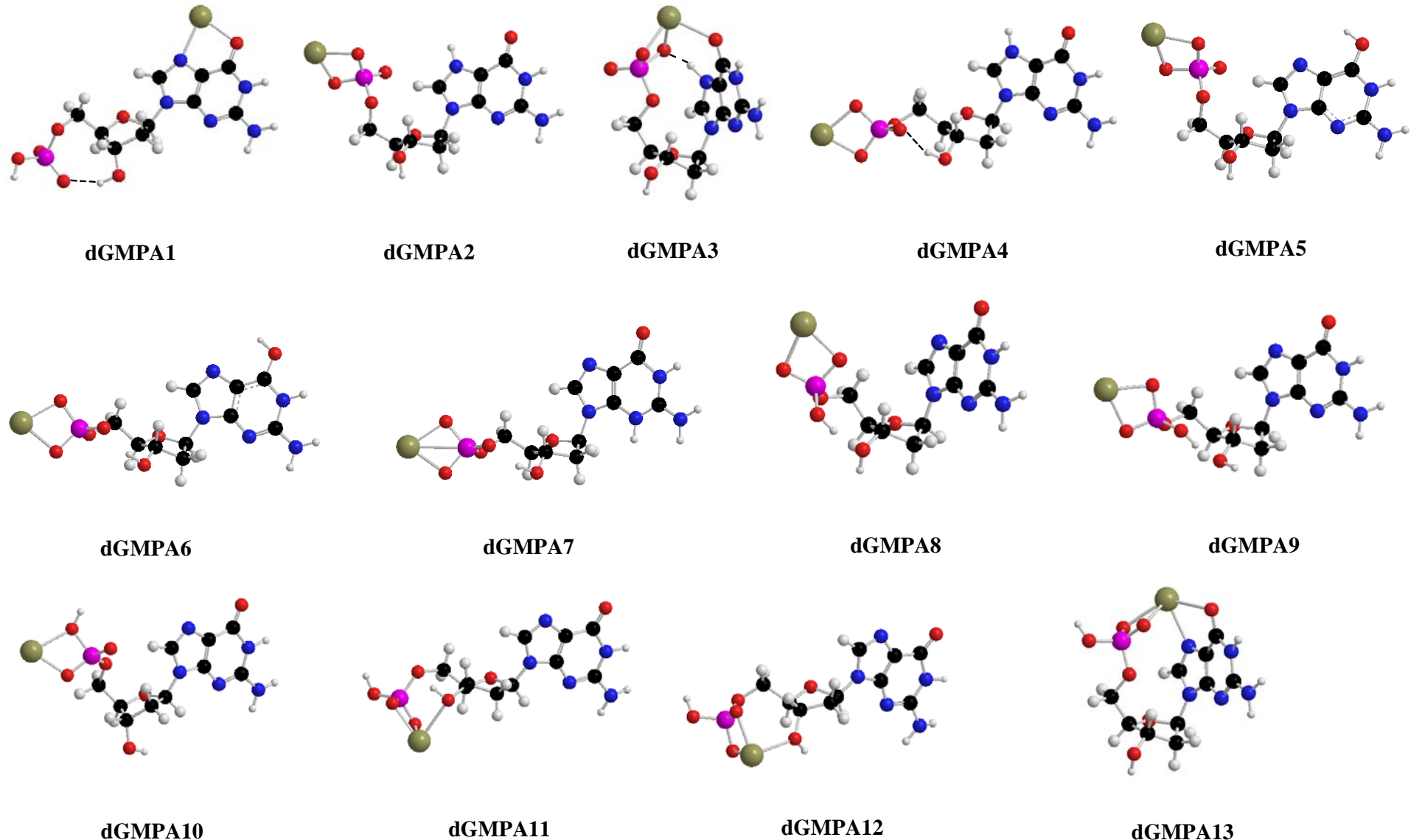
5S. Evolution of [Pb(dGMP)-H]⁺ arrival time as a function of 1/E, the electric field applied across the mobility tube.

1S. Low energy CID spectrum of the $[\text{Pb}(\text{GMP})\text{-H}]^+$ complex recorded at 30 eV (laboratory frame).

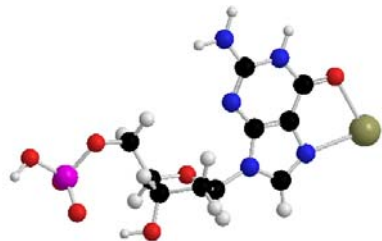


2S. Structure and geometrical details of the various structures optimized for the $[\text{Pb}(\text{dGMP})\text{-H}]^+$ complex

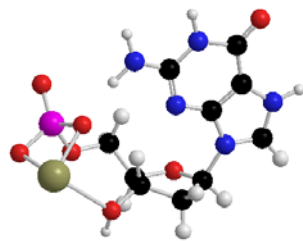
2.1 Anti forms



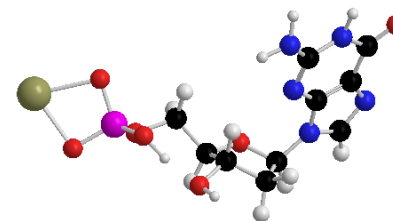
2.2 Syn forms



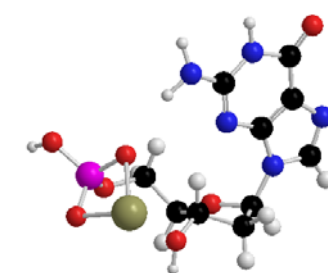
dGMPS1



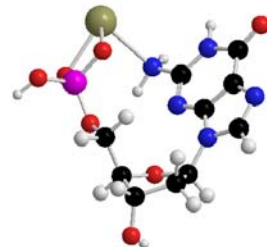
dGMPS2



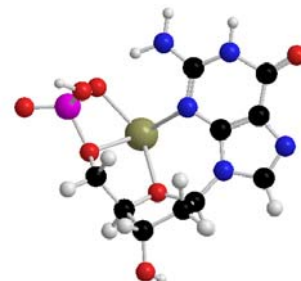
dGMPS3



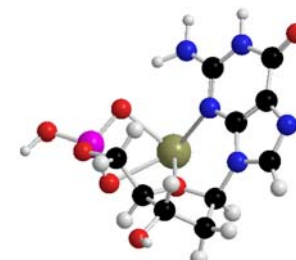
dGMPS4



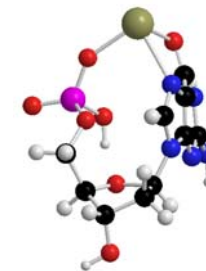
dGMPS5



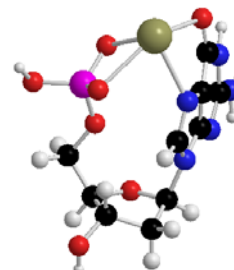
dGMPS6



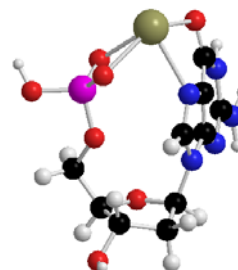
dGMPS7



dGMPS8



dGMPS9



dGMPS10

2.3 Summary

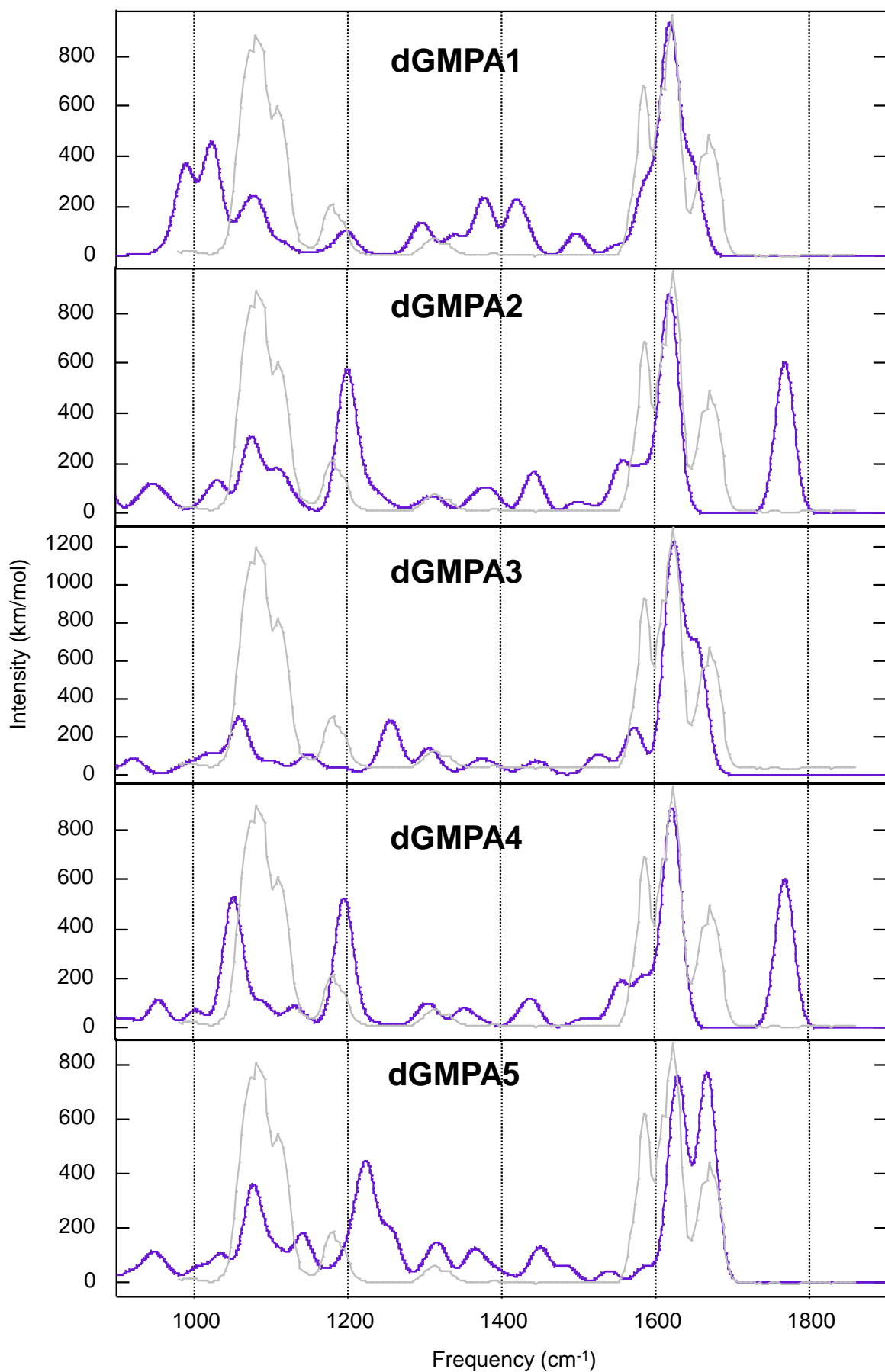
Structures	Interaction sites								Sugar conformation ^(a)	Intramolecular H bonds	
	Phosphate	O4'	OH 3'	OH 5'	C=O (6)	NH ₂	N1	N3	N7		
Anti forms											
dGMPA1					○				○	C2'-endo/C1'-exo (² T ₁)	
dGMPA2	○ (O/O)									C3'-endo/C2'-exo (³ T ₂)	
dGMPA3	○ (O/O)				○					C3'-endo/C2'-exo (³ T ₂)	NH(7)→ Phos
dGMPA4	○ (O/O)									C3'-endo (³ E)	OH(3')→ Phos
dGMPA5	○ (O/O)									C3'-endo/C2'-exo (³ T ₂)	
dGMPA6	○ (O/O)									C3'-endo (³ E)	OH(3')→ Phos
dGMPA7	○ (O/O)									C3'-endo/C2'-exo (³ T ₂)	OH(3')→ Phos
dGMPA8	○ (O/O)									C3'-endo/C2'-exo (³ T ₂)	Phos → OH(3')
dGMPA9	○ (O/O)									C3'-endo/C2'-exo (³ T ₂)	Phos → OH(3')
dGMPA10	○ (O/OH)									C2'-endo/C3'-exo (² T ₃)	
dGMPA11	○ (O/O)		○							C3'-endo/C4'-exo (³ T ₄)	
dGMPA12	○ (O/O)		○							O4'-endo/C1'-exo (⁰ T ₁)	
dGMPA13	○ (O/O)				○				○	C3'-endo/C2'-exo (³ T ₂)	
Syn forms											
dGMPS1					○				○	C2'-endo/C1'-exo (² T ₁)	OH(3')→ Phos
dGMPS2	○ (O/O)		○							C3'-endo/C2'-exo (³ T ₂)	
dGMPS3	○ (O/O)									C3'-endo/C2'-exo (³ T ₂)	Phos → OH(3')
dGMPS4	○ (O/O)		○							C3'-endo/C2'-exo (³ T ₂)	
dGMPS5	○ (O/O)					○				C2'-endo/C3'-exo (² T ₃)	
dGMPS6	○ (O)	○		○				○		C2'-endo/C3'-exo (² T ₃)	
dGMPS7	○ (O/O)	○						○		C3'-endo/C2'-exo (³ T ₂)	
dGMPS8	○ (O)				○				○	C2'-endo/C3'-exo (² T ₃)	Phos → O (4')
dGMPS9	○ (O/O)				○				○	C3'-endo/C2'-exo (³ T ₂)	
dGMPS10	○ (O/O)				○				○	C3'-endo/C2'-exo (³ T ₂)	

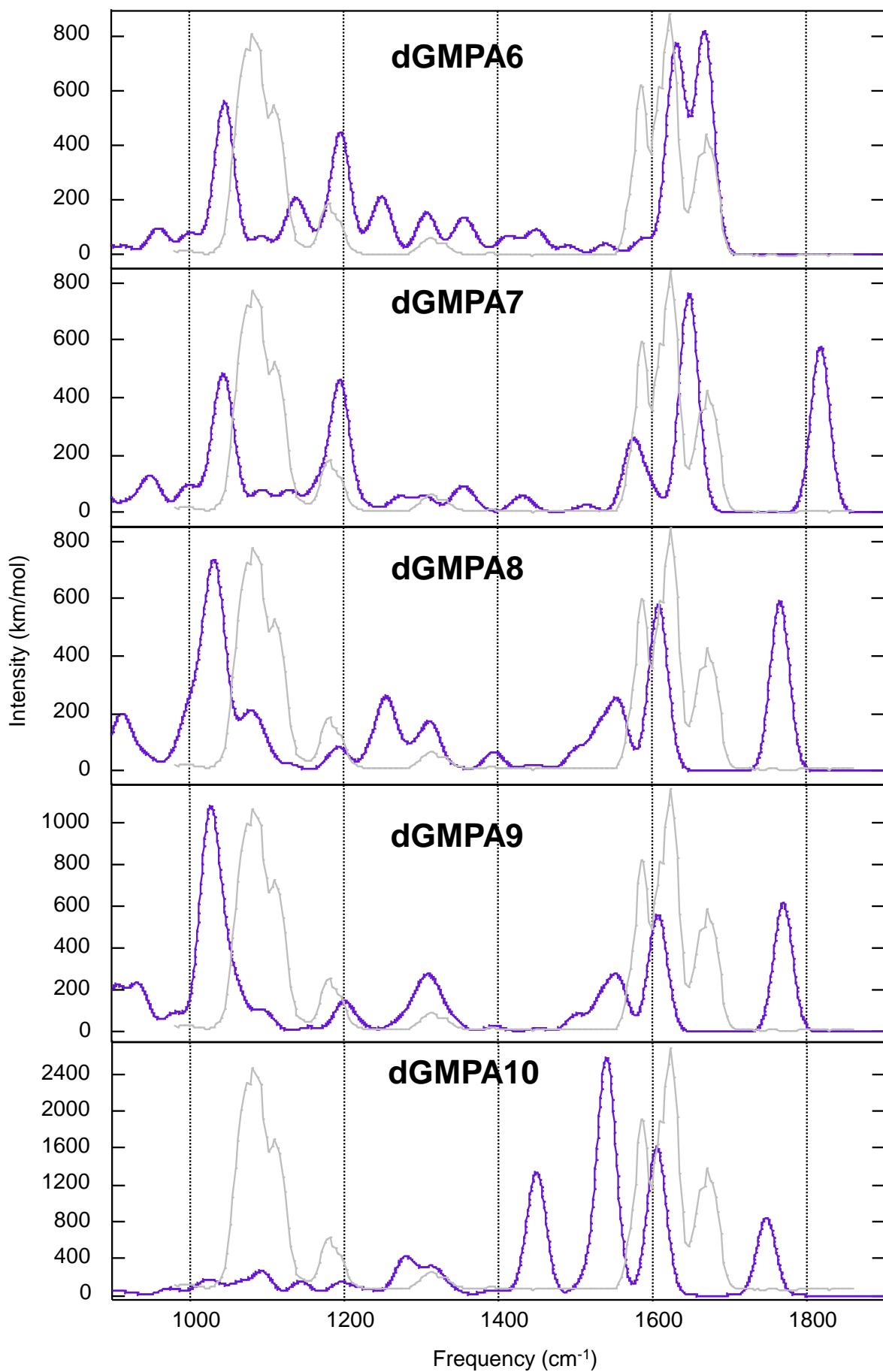
(a) Four ring atoms are considered as planar (E forms) when their associated torsional angle is greater than 179°

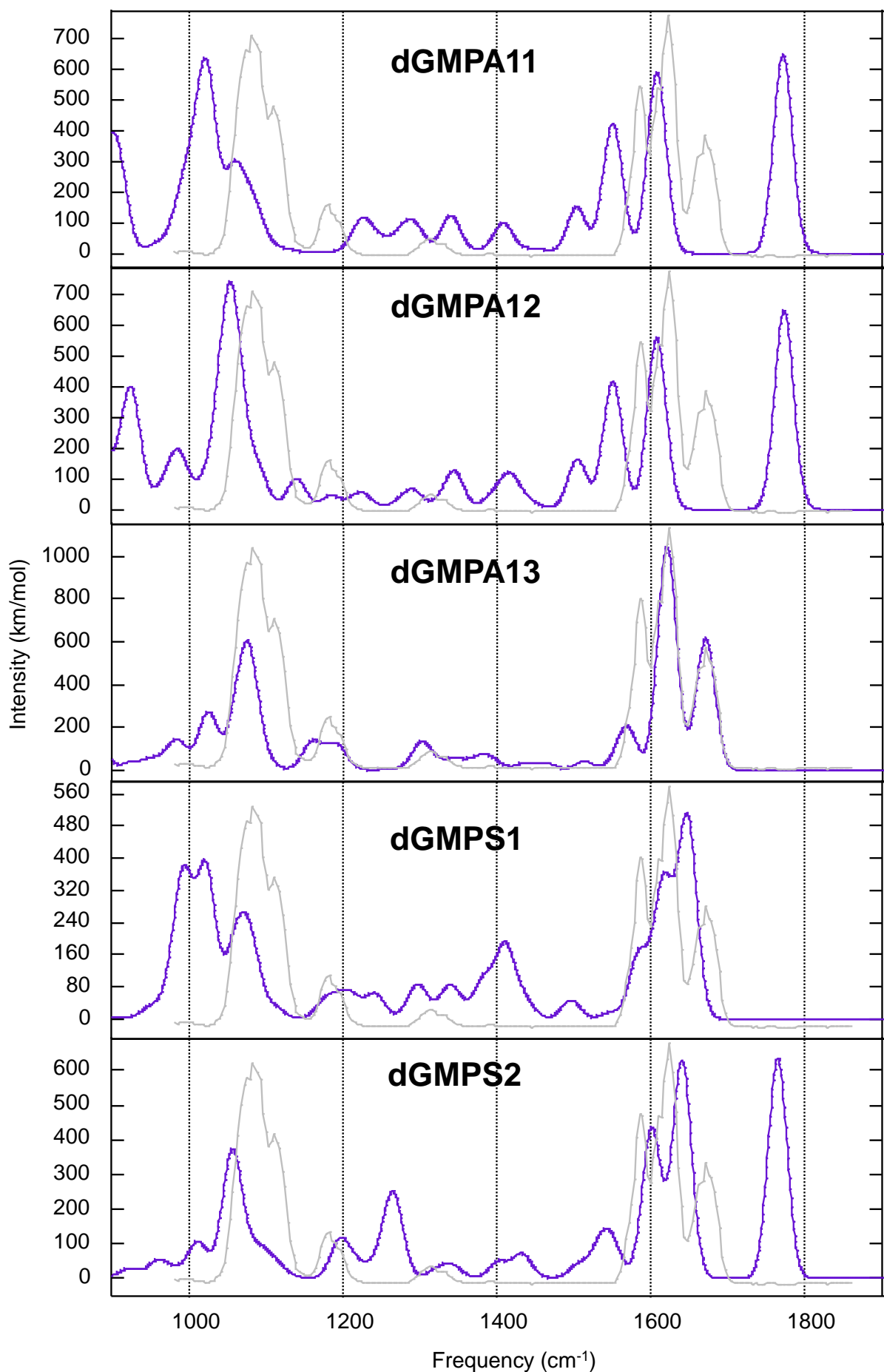
3S. Total energy, thermal correction to Gibbs free energy (TCG) and ZPE (Hartree) of the various structures considered during this study.

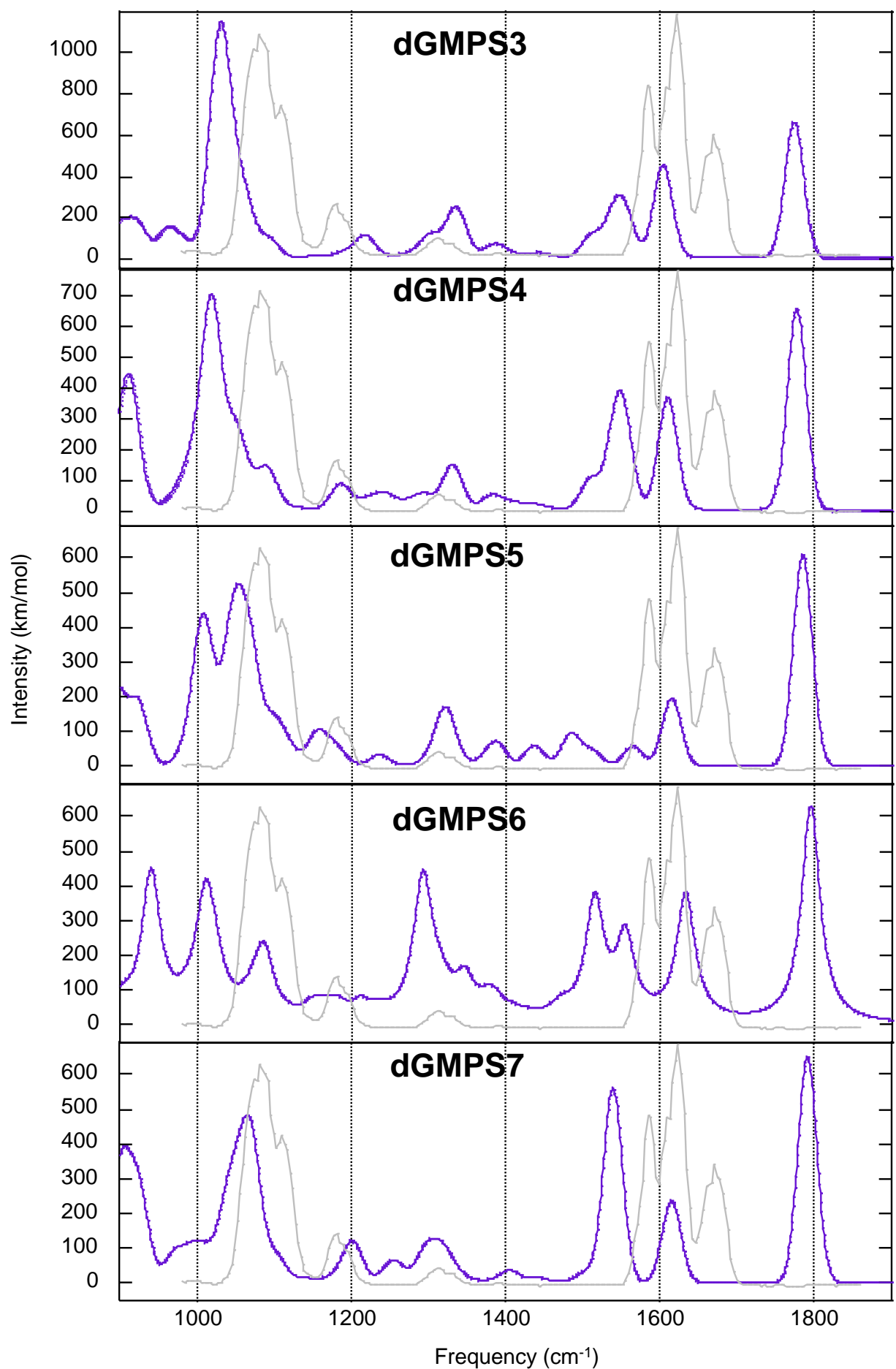
Structure	B3LYP/6-31G(d,p)			B3LYP//6-311+G(2df,2p)
	E	ZPE	TCG	E
dGMPA1	-1533.845199	0.266534	0.209900	-1534.329415
dGMPA2	-1533.956524	0.268431	0.212373	-1534.443255
dGMPA3	-1533.955654	0.267647	0.216837	-1534.434760
dGMPA4	-1533.951044	0.269049	0.212966	-1534.437542
dGMPA5	-1533.930100	0.268004	0.211968	-1534.41654
dGMPA6	-1533.93549	0.268700	0.212493	-1534.421218
dGMPA7	-1533.917473	0.267758	0.211300	-1534.404346
dGMPA8	-1533.928523	0.268243	0.213293	-1534.414012
dGMPA9	-1533.928081	0.267856	0.211509	-1534.414562
dGMPA10	-1533.881039	0.265704	0.206523	
dGMPA11	-1533.929477	0.266978	0.211334	-1534.414943
dGMPA12	-1533.93568	0.266842	0.211183	-1534.422404
dGMPA13	-1533.993128	0.268303	0.216814	-1534.475306
dGMPS1	-1533.841038	0.266733	0.210618	
dGMPS2	-1533.951487	0.269717	0.218234	-1534.431864
dGMPS3	-1533.929210	0.267705	0.212417	-1534.416566
dGMPS4	-1533.942752	0.267361	0.214402	-1534.425433
dGMPS5	-1533.928814	0.267843	0.214730	-1534.412366
dGMPS6	-1533.945020	0.267200	0.214716	-1534.424076
dGMPS7	-1533.961591	0.267712	0.215996	-1534.442794
dGMPS8	-1533.965819	0.268626	0.217449	-1534.448121
dGMPS9	-1533.987905	0.268021	0.215972	-1534.471506
dGMPS10	-1533.989783	0.267613	0.215146	-1534.474311

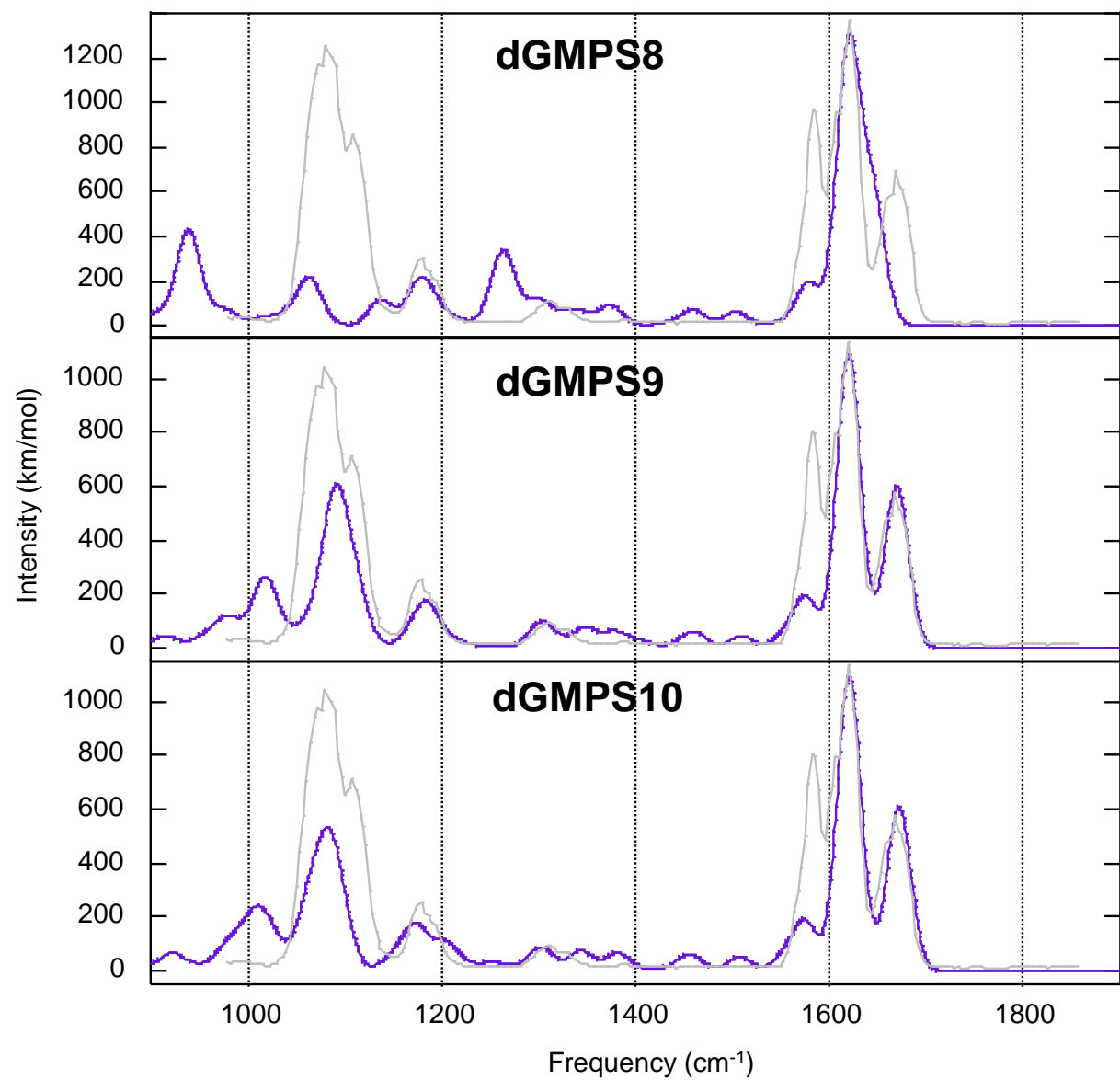
4S. DFT-computed IR absorption spectra for the $[\text{Pb}(\text{dGMP})\text{-H}]^+$ structures. The experimental IRMPD spectrum is overlayed in grey.











5S. Evolution of $[\text{Pb}(\text{dGMP})\text{-H}]^+$ drift time as a function of $1/E$, E the electric field applied across the mobility tube. Inset shows a drift time distribution at $E = 700\text{V/m}$ (blue) overlaid with the expected distribution (red) for a single conformation in the same experimental conditions. The expected distribution for CCS 10% higher (dashed green) is well separated, showing that only one family of conformations is observed experimentally. From the slope can be deduced the collisional cross section of the main conformation of $[\text{Pb}(\text{dGMP})\text{-H}]^+$ in the gas phase : 99.6\AA^2

